Current Biology 17, 1396–1402, August 21, 2007 ©2007 Elsevier Ltd All rights reserved DOI 10.1016/j.cub.2007.07.020

Report

Abscisic Acid Triggers the Endocytosis of the *Arabidopsis* KAT1 K^+ Channel and Its Recycling to the Plasma Membrane

Jens-Uwe Sutter,[1] Christian Sieben,[2] Andreas Hartel,[2] Cornelia Eisenach,[1] Gerhard Thiel,[2] and Michael R. Blatt[1,*]

[1] Laboratory of Plant Physiology and Biophysics
IBLS - Plant Sciences
Bower Building
University of Glasgow
Glasgow G12 8QQ
United Kingdom

[2] Botanisches Institut
Universität Darmstadt
Schnittspahnstrasse 1-3
D64287 Darmstadt
Germany

Summary

Membrane vesicle traffic to and from the plasma membrane is essential for cellular homeostasis in all eukaryotes [1–3]. In plants, constitutive traffic to and from the plasma membrane has been implicated in maintaining the population of integral plasma-membrane proteins and its adjustment to a variety of hormonal and environmental stimuli [2, 3]. However, direct evidence for evoked and selective traffic has been lacking. Here, we report that the hormone abscisic acid (ABA), which controls ion transport and transpiration in plants under water stress [4, 5], triggers the selective endocytosis of the KAT1 K^+ channel protein in epidermal and guard cells. Endocytosis of the K^+ channel from the plasma membrane initiates in concert with changes in K^+ channel activities evoked by ABA and leads to sequestration of the K^+ channel within an endosomal membrane pool that recycles back to the plasma membrane over a period of hours. Selective K^+ channel endocytosis, sequestration, and recycling demonstrates a tight and dynamic control of the population of K^+ channels at the plasma membrane as part of a key plant signaling and response mechanism, and the observations point to a role for channel traffic in adaptive changes in the capacity for osmotic solute flux of stomatal guard cells [5, 6].

Results and Discussion

To explore the dynamics of the KAT1 K^+ channel in abscisic acid (ABA), we took advantage of GFP fluorescence—and that of a photoactivatable variant (paGFP)—to monitor movement of tagged KAT1 proteins [7] expressed in tobacco epidermal and guard cells. ABA controls the gating of guard cell K^+ and Cl^- channels—among these the KAT1 K^+ channel of *Arabidopsis* and its homologs in tobacco and *Vicia*—to promote osmotic solute efflux, close stomata, and prevent transpirational water loss from plant leaves in response to water stress [4, 5, 8]. ABA is associated with adaptive changes, notably in the capacity for solute flux in guard cells [6] and their ability to retain a "memory" of stress [9], implying selective alterations in the population of functional transporters at the plasma membrane. ABA also regulates ion transport in other tissues, including roots, epidermal, and mesophyll cells [10–12]. Previous studies uncovered a role for the membrane trafficking proteins NtSyp121 from tobacco and its *Arabidopsis* homolog AtSyp121 in the distribution and anchoring of the KAT1 K^+ channel within the plasma membrane [7]. NtSyp121 and AtSyp121 are members of the superfamily of SNAREs (soluble NSF [*N*-ethylmaleimide-sensitive factor] attachment protein receptors) that drive membrane traffic in all eukaryotes [1–3]. NtSyp121 and AtSyp121 act late in the secretory pathway to the plasma membrane, and disrupting their activity affects secretory traffic and cellular development [13] and suppresses the regulation by ABA of guard cell K^+ and Cl^- channels [14]. Of these, the KAT1 K^+ channel localizes to microdomains at the plasma-membrane surface [7]. This organization is affected by the SNAREs [7] and, thus, might underpin ABA-mediated control of the K^+ channels.

ABA Triggers KAT1 K^+ Channel Internalization

Figures 1A and 1B summarize results from one experiment with confocal images taken at 5 min intervals throughout to minimize photobleaching (see also Movies S1–S3 in the Supplemental Data available online). The same patterns of fluorescence redistribution were obtained in each of ten other experiments and with guard cells expressing the tagged KAT1 constructs after biolistic transfection (Figures 1C and 2B). As before [7], KAT1 was distributed in discrete, positionally stable microdomains at the cell perimeter before ABA treatments. In no case was KAT1 fluorescence observed within endomembrane compartments that would suggest a mistargeting from overexpression (see also Sutter et al. [3]). After adding ABA, however, this distribution pattern was generally lost within 10–20 min, leaving a mobile and diffuse fluorescence around the cell periphery; after 30 min in ABA, GFP fluorescence was strongest in mobile structures moving in and out of transvacuolar cytoplasmic strands (see Movie S5). We examined the lateral mobility of this diffuse pattern by fluorescence recovery after photobleaching (FRAP) with 488 nm light. Unlike control experiments before ABA treatments, when photobleaching was carried out 30–60 min after adding ABA, the local fluorescence recovered within 60 s of photobleaching (Figure S4, Movies S4 and S5), indicating a high mobility of the tagged K^+ channel within the cytoplasm [7]. Control experiments, adding 20 μM K^+-acetate in place of ABA, showed a progressive photobleaching (see Figure 2C) as expected, but offered no evidence for loss in

*Correspondence: m.blatt@bio.gla.ac.uk

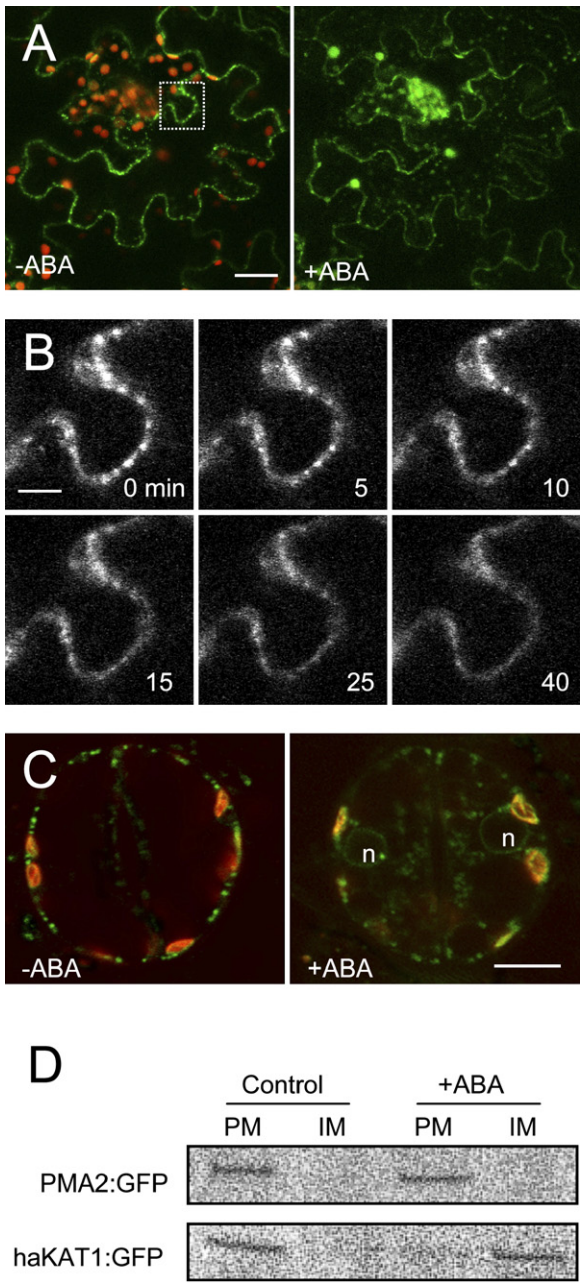

Figure 1. ABA Evokes K⁺ Channel Internalization in Tobacco Epidermis and Guard Cells and Its Recovery in Endosomal Compartments

(A) Three-dimensional reconstructions of one tobacco epidermal cell expressing haKAT1-GFP before (−ABA) and 60 min after (+ABA) adding 20 μM ABA show a loss of the GFP fluorescence signal from the KAT1 microdomains at the cell periphery. Similar results obtained with 1 μM ABA (not shown). Image stacks collected at 5 min intervals to give deep sections within the epidermal cell layer parallel to the leaf surface (see also Movies S1 and S2). Boxed area refers to image frames in (B). Chloroplasts (in red) show enhanced fluorescence in the GFP channel after repeated excitation with 488 nm light. Similar results were obtained in 10 independent experiments, in single-plane image series taken at 2 and 3 min intervals and with photoactivation of haKAT1-paGFP.

(B) Three-dimensional image frames of the same epidermal cell area (above) showing KAT1 microdomains and time course (in min) of K⁺ channel withdrawal therefrom.

(C) Central sections through one guard cell pair expressing haKAT1-GFP before (−ABA) and 60 min after (+ABA) adding 20 μM ABA. Similar results obtained with 1 μM ABA (not shown). Note the nuclear ring, cytoplasmic strands, and internal labeling in ABA and the corresponding loss of KAT1 microdomains from the cell periphery. The small decrease in stomatal aperture apparent in these images is unlikely to reflect the true change in response to ABA, because reliable estimates based on fluorescence images require the use of extracellular or peripheral markers and three-dimensional reconstructions [39, 40]. Measurements taken from brightfield images indicated a normal stomatal response to ABA after KAT1 expression (see Figure S1). Scale bars represent 20 μm (A), 5 μm (B), and 10 μm (C).

(D) Western blot analysis (10 μg total protein/lane) of the H⁺-ATPase (PMA2-GFP) and KAT1 K⁺ channel (haKAT1-GFP) localization expressed in tobacco leaves alone (Control) and after 60 min in ABA (+ABA). Solubilized microsomal membranes separated by two-phase partitioning between plasma membrane (PM) and endomembrane (IM) fractions. Proteins separated by SDS-PAGE. Western blots probed with polyclonal antibody to GFP and HA and visualized by radiotracer phosphoimaging.

microdomain structure or fluorophore dispersion (not shown). Parallel western blot analyes, carried out after isolating microsomes and two-phase partitioning (Figure 1D), showed the K⁺ channel (HA) epitope almost exclusively in the plasma membrane fraction in the absence of ABA, consistent with previous results [7]. However, the K⁺ channel was found primarily within endomembrane fractions when leaf sections were harvested 60 min after infiltration with 20 μM ABA. In neither case was GFP- or HA-antibody binding found in the soluble fractions (not shown), ruling out degradation.

K⁺ Channel Endocytosis Initiates without Delay and Is Selective

We made use of kymographic analysis, recording the fluorescence signal around the periphery of each cell to quantify KAT1 internalization. The results (Figure 2) supported visual inspections showing stationary domains of high fluorescence with a common discontinuity and decay upon addition of ABA, thus discounting a spreading of the K⁺ channel microdomains in ABA. We extracted kymograph segments corresponding to KAT1 microdomains to determine the relaxation kinetics. In every case, the fluorescence decay was well fitted as a single exponential decay, and within any one experiment virtually identical results were obtained from each microdomain (Figure 2C), yielding a mean halftime of 11 ± 3 min. Extrapolating the fitted curves to the initial fluorescence signal recorded prior to adding ABA also yielded initial lag times (1.8 ± 0.1 min) similar to the period required for solution exchange in the chamber (1.6 ± 0.1 min, n = 5), indicating that KAT1 internalization began within 20 s of ABA delivery.

To test whether KAT1 internalization was selective, we examined the fluorescence distribution and mobility of the GFP-tagged PMA2 H⁺-ATPase from *Nicotiana plumbaginifolia*. The H⁺-ATPase yields uniform GFP fluorescence at the cell surface [7, 15], with no evidence of the exclusion zones reported for the yeast H⁺-ATPase [16] and, like KAT1, is found in detergent-resistent membrane fractions [7, 17, 18]. So, it is likely that the submicroscopic distributions of these membrane proteins overlap. Unlike KAT1, ABA had no effect on PMA2-GFP distribution, even after 120 min exposure. Instead, the H⁺-ATPase was uniformly distributed at the cell perimeter without the appearance of internal structures

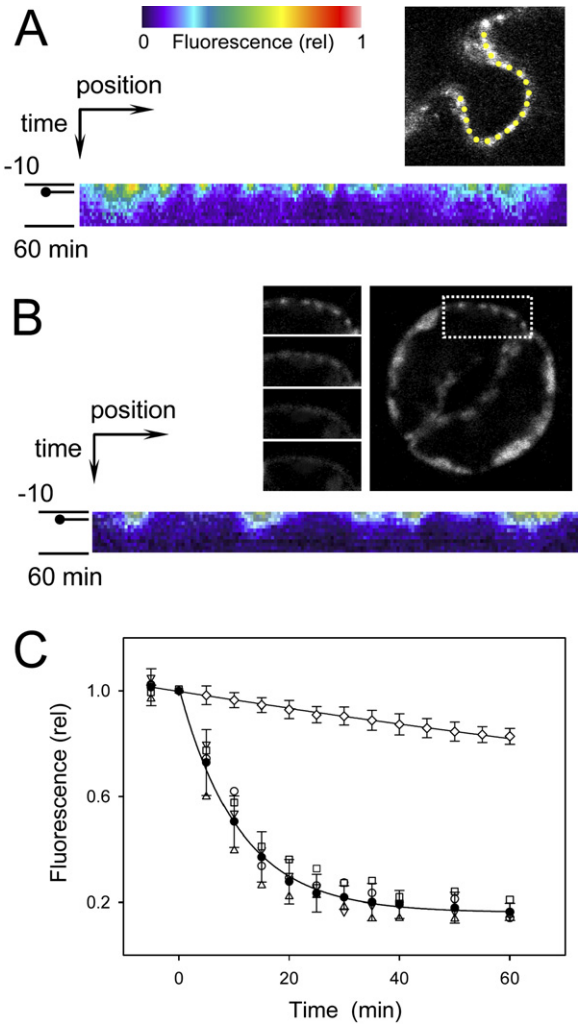

Figure 2. ABA Mobilizes the KAT1 K^+ Channel from Plasma Membrane Microdomains

(A) Kymographic analysis of KAT1 fluorescence from Figure 1B taken over the time course of the experiment from pixels along a line traced around the edge of the cell (dotted line, inset) and averaged over a width of 10 pixels (~1.4 μm). Similar results were obtained with line widths of 3, 5, and 8 pixels (0.5–1.0 μm). Position along the line determines the horizontal axis, time progresses downward, and fluorescence intensity is color coded (scale above). Time of ABA addition indicated on the left (lollipop).

(B) Similar kymographic analysis of KAT1 fluorescence decay from one guard cell pair. The region of analysis (insets) taken to avoid the fluorescence from chloroplasts around the cell periphery and lip of the stomatal pore. Note the loss of fluorescence in ABA without evidence of filling or lateral movement near the edges of the microdomains (compare Figures 4 and 8 in Sutter et al. [7]).

(C) Microdomain fluorescence decay with ABA addition (at t = 0). Fluorescence normalized to time of ABA addition and shown for four individual microdomains (open symbols) and as means ± SE (closed circle) of data from six independent experiments (epidermal and guard cells). Data fitted by nonlinear least-squares as a single-exponential decay (halftime, 11 ± 3 min). Normalized means ± SE of three experiments imaged with the same settings and addition of 20 μM acetate (open diamond) indicates the time course of fluorescence bleaching.

(see Movie S6), and FRAP analysis indicated no significant mobility in ABA (not shown), much as was observed before without ABA [7]. Finally, western blot analysis after two-phase partitioning showed that the H^+-ATPase (GFP) epitope was recovered almost exclusively in the plasma membrane fraction both before and 60 min after adding ABA (Figure 1D). Thus, both the image and biochemical studies lead us to conclude that ABA triggers the selective internalization of KAT1 from the plasma membrane.

KAT1 Is Sequestered in an Endosomal Pool for Recycling to the Plasma Membrane

The recovery of KAT1 after ABA treatments in inner membrane fractions and within internal cytoplasmic structures prompted us to explore their nature in dual-labeling studies. We used FM4-64 as a marker for endocytosis [19–21] and coexpressed selected YFP-tagged proteins to test for colocalization within degradative and associated endosomal pathways. Internal haKAT1-GFP labeling was found to colocalize with FM4-64 (Figure 3A), consistent with vesicular endocytosis of KAT1 and its recovery in inner membrane fractions (Figure 1D). By contrast, whereas some overlap between the endosomal and KAT1 markers was seen, no consistent pattern of colocalization was visible either with the Golgi marker sialyl-transferase-YFP (not shown) or with BP80-YFP, a marker for the Golgi and prevacuolar compartment [22] (Figure 3B). Similarly, no consistent colocalization was evident with YFP-tagged FYVE domain peptide (Figure 3C) or with ARA7-YFP (Figure 3D), which label early endosomes and the lytic pathway to the vacuole [20, 23, 24]. Instead, the overwhelming pattern was of noncoincidence between markers, indicating that KAT1 is sequestered in a separate, as-yet-unidentified endomembrane compartment.

Because K^+ channel traffic offers a potential mechanism for post-translational regulation of K^+ flux capacity, we were interested to test whether, once sequestered, KAT1 recycled to the plasma membrane. For this purpose, we took advantage of paGFP photoactivation to monitor haKAT1-paGFP redistribution from the endosomes after ABA washout.We anticipated that if KAT1 was recycled to the plasma membrane, then K^+ channels photoactivated after internalization should be recovered in nonmobile, fluorescent microdomains at the cell periphery after ABA washout. Use of paGFP ensured that any fluorescence recovered in microdomains will have had to come from those KAT1 proteins photoactivated at the end of the ABA treatment. By the same reasoning, it was expected that internalized GFP fluorescence should reform in microdomains, even when de novo protein synthesis was blocked. Thus, in separate experiments, we monitored haKAT1-GFP distributions after pretreatment with 20 μM ABA for 60 min and in 300 μM cycloheximide. Additionally, we used FRAP to check the recovery of positionally stable microdomains at the plasma membrane [7]. Finally, we carried out western blot analysis after two-phase partitioning of transfected leaves infiltrated with ABA for 1 hr and subsequently washed by infiltrations with cycloheximide alone (see Experimental Procedures). All four strategies yielded complementary results. After ABA pretreatments, photoactivation and conventional GFP fluorescence indicated the predominant distribution of KAT1 in mobile endosomes, both in guard cells and in epidermal cells, and the fluorescent signal was recovered in peripheral microdomains after 6–8 hr superfusion

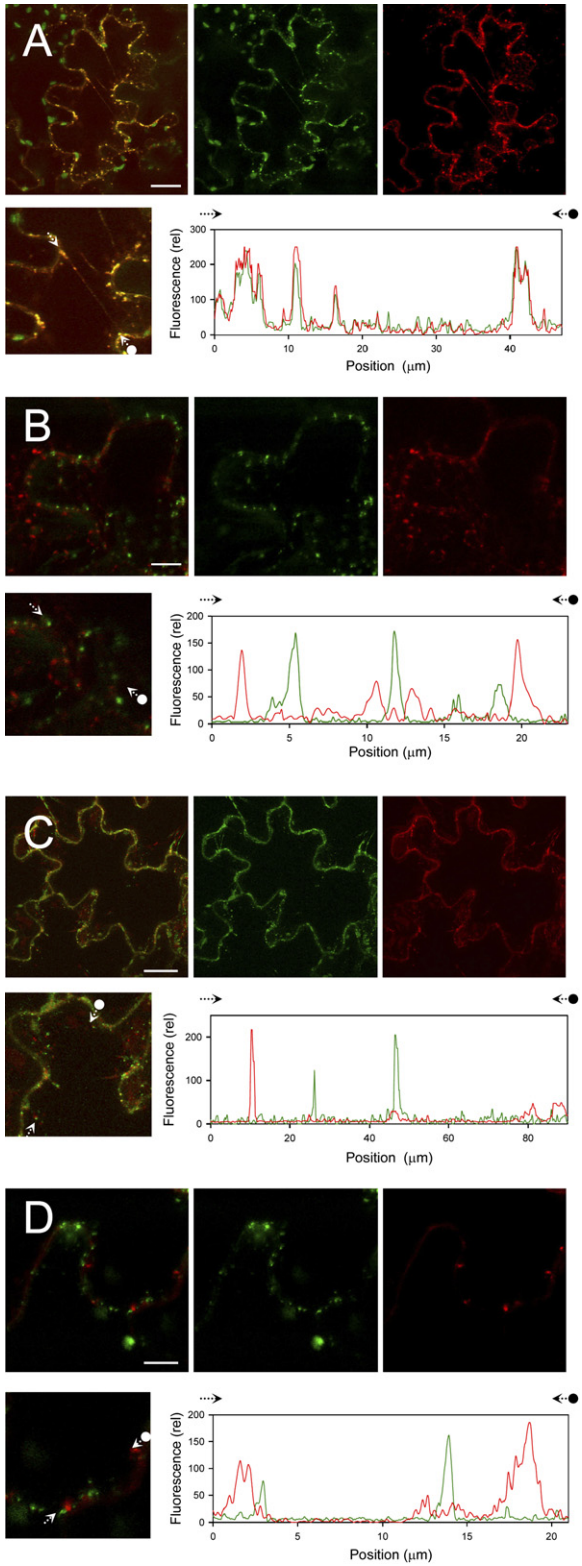

Figure 3. KAT1 K⁺ Channels Localize together with FM4-64 Internalized from the Plasma Membrane but Do Not Colocalize with Markers for Early Endosomes and the Lytic Pathway to the Vacuole

For clarity, images are three-dimensional reconstructions of stacks through the epidermis omitting the outer and inner cell surfaces and parallel to the leaf surface, in each case with (left to right) overlay, GFP, and YFP/FM4-64 channels. Similar results obtained in at least three independent experiments in each case and at time points 1–3 hr in the presence of 20 μM ABA.

(A) Tobacco epidermal cells expressing haKAT1-GFP labeled with 5 μM FM4-64 for 5 min prior to adding 20 μM ABA for 60 min shows uniform coincidence of the internalized K⁺ channel marker with FM4-64.

(B–D) haKAT1-GFP coexpressed with BP80-YFP (B), YFP-tagged FYVE domain peptide (C), and ARA7-YFP (D) as markers for the Golgi apparatus, the prevacuolar compartment [22], and for early endosomes [20, 23, 41], respectively. See also Movies S8–S11. Line scan analyses (beginning and end of line scans as indicated in thumbnails) taken along cytoplasmic strands to avoid the cell periphery and show a general noncoincidence with these markers. Scale bars represent 20 μm (A), 50 μm (C), and 10 μm (B and D).

without ABA (Figure 4 and Figures S2 and S3); FRAP analyses (Figure S4 and Movie S7) showed a coincident recovery of positional stability to the microdomains and a loss of mobile, internal fluorescent compartments; finally, western blot analysis of leaf tissues taken 8 hr after ABA washout showed that the K⁺ channel was found almost entirely in the plasma membrane fraction (compare Figure 4D and Figure 1D). Thus, the KAT1 K⁺ channel is recycled to the plasma membrane after ABA washout.

Evoked Traffic in Dynamic K⁺ Channel Control

The results outlined above establish the principle and demonstrate the dynamics of hormonally evoked and selective traffic for an integral plasma membrane protein in plants. They provide direct evidence for a triggered endocytosis and for recycling of the KAT1 K⁺ channel from the plasma membrane, events that are initiated in parallel with changes in K⁺ channel activities known to be evoked by ABA [4, 5, 8]. We interpret this sequestration and recycling in the context of adaptive modulation of the K⁺ channel population at the plasma membrane. In guard cells, ABA triggers the activation of Cl^- channels and inactivation of inward-rectifying K⁺ channels, notably KAT1, within the 30–60 s of exposure, changes that are mediated through cellular signals, including elevated cytosolic-free [Ca^{2+}] [4, 5, 8]. Significantly, the time course for these events is roughly one order of magnitude less ($t_{1/2}$, 20−30 s) than for KAT1 endocytosis. Even in barley roots, for which the time course for response has been partially characterized by electrophysiological means [10], ABA evokes changes in K⁺ transport that are faster than that KAT1 endocytosis. However, KAT1 sequestration and recycling accords with longer-term changes in channel activities [12] and solute flux capacity [6], and with so-called programmed closure of stomata, a delayed reopening that is manifest over several hours after cytosolic-free [Ca^{2+}] elevation [9].

Electrophysiological studies have yet to address the question of K⁺ channel recovery from ABA and water stress. Nonetheless, we note that the expression of many K⁺ channels—notably in guard cells [25]—is surprisingly insensitive to drought and ABA, implying an important role for ion channel exchange with endomembrane pools for long-term adaptive control. By contrast, guard cell Cl^- channel activities respond and recover their resting activity within 1–3 min of ABA addition and washout [26], supporting the idea of a selective traffic of the K⁺ channels. These characteristics are

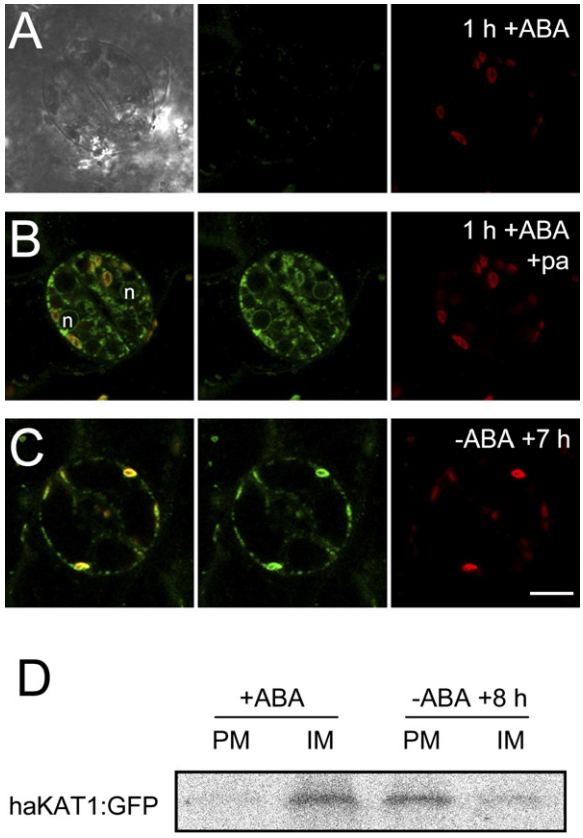

Figure 4. KAT1 K^+ Channels Recycle to Plasma Membrane-Localized Microdomains

(A–C) Three-dimensional reconstructions (for clarity, omitting upper and lower surfaces) of tobacco guard cells expressing haKAT1-paGFP and pretreated with 20 μM ABA for 60 min. Image sets taken (A) before and (B) after photoactivation (±pa) at the start of ABA washout, and (C) after a further 7 hr continuous superfusion with buffer −ABA (see also Figures S2–S4 and Movies S4, S5, and S7). Images are (left to right) overlay, GFP, and chloroplast (red) channels. Brightfield image overlay included in (A). Nuclei (n) are labeled in (B). Chloroplasts within the stomatal pore in (C) are the consequence of cell debris accumulating during continuous perfusion. Similar results obtained in three independent experiments. Scale bar represents 20 μm.

(D) Western blot analysis (10 μg total protein/lane) of KAT1 K^+ channel (haKAT1-GFP) localization expressed in tobacco leaves 60 min after perfusion with ABA and 300 μM cycloheximide (+ABA), and 8 hr after subsequent perfusion with 300 μM cycloheximide alone (−ABA +8 h). Solubilized microsomal membranes separated by two-phase partitioning between plasma membrane (PM) and endomembrane (IM) fractions. Proteins separated by SDS-PAGE and western blot probed with polyclonal primary antibody to HA and visualized by radiotracer phosphoimaging.

similar to those for cycling of glucose transporters to and from the mammalian epithelial plasma membrane in response to insulin [27] but, to date, find no parallels with membrane traffic in plants or fungi. Indeed, direct evidence has been lacking for evoked membrane traffic, especially of ion channels, although it has been proposed that ion-channel traffic in plants is subject to hormonal and environmental control [2, 3]. Previous studies have identified changes in the constitutive traffic of a number of plasma membrane proteins in plants leading to their degradation [21, 28–30]. However, even for PIN1, a putative auxin transporter, auxin itself affects only a steady-state turnover at the plasma membrane [31]. Furthermore, none of these studies provide information about the kinetics of traffic beyond endpoint determinations.

It is of interest that ABA triggers KAT1 endocytosis when the channel is expressed in epidermal cells as well as guard cells. Although the transport characteristics of the leaf epidermis has yet to be examined in any detail, ABA is known to affect ion activities of cells both of the stomatal complex and of the neighboring epidermis [32, 33]. ABA also regulates ion transport in other tissues, including roots and mesophyll cells [10–12]. We note, too, that KAT1 expression in *Arabidopsis* is not restricted to guard cells [25]. Thus, it appears that KAT1 is capable of engaging within parallel trafficking events triggered by the hormone in these cells. That ABA selectively mobilizes the KAT1 K^+ channel but not the H^+-ATPase from the plasma membrane is especially intriguing and implies a focused recruitment for endocytosis—plausibly targeted to the microdomains [19]—because both proteins are found in detergent-resistent membrane fractions and their distributions at the plasma membrane appear to overlap [7, 18]. Thus, KAT1 internalisation is not simply the consequence of bulk endocytosis during a decrease in cell-surface area, such as is associated with stomatal closure, and it contrasts with K^+ channel traffic during osmotically driven changes in volume that maintains transporter population densities rather than a targeting specific transport proteins [19].

One of the most intriguing features of KAT1 is its localization within 0.5–0.6 μm diameter microdomains at the plasma membrane surface [7]. KAT1 clustering is consistent with electrophysiological evidence for nonhomogeneous distributions of many ion channels [34], including K^+ channels of guard cells [19], and accords with evidence for channel-associated trafficking and scaffolding protein complexes [35, 36]. The microdomains of KAT1 K^+ channels are remarkably constant spatially, and this stability appears important for their regulation [7]. Although we cannot exclude the possibility of an anomalous KAT1 distribution—plant ion channels normally express at levels that are too low for detection by GFP fluorescence or protein biochemistry—35S-driven expression commonly aligns closely with that of the native protein [37], and only with extreme overexpression does KAT1 accumulate in the secretory pathway [7]. In fact, KAT1 clustering appears species and tissue independent [7, 19] and thus may couple to common signaling pathways with ABA in each case [5, 8].

Finally, our data bear witness to a role for K^+ channel traffic that differs from the control of channel gating by ABA. This last point is especially important because it gives substance to the idea that the SNAREs NtSyp121 and AtSyp121 contribute to cell signaling by controlling ion-channel activities in ways that are distinct from their functions in vesicle trafficking. Work from this laboratory [14] first implicated a role for these SNAREs in ABA signaling after electrophysiological studies demonstrated that NtSyp121 is required for early, ABA-mediated control of K^+ and Cl^- channels at the plasma membrane. In the absence of further knowledge, these observations left open questions about the relationship between the SNAREs, K^+ and Cl^- channel regulation, whether

mediated through ion-channel trafficking or through protein interactions within the plasma membrane. Our present results are difficult to reconcile with the rapid inactivation of KAT1 and of similar inward-rectifying K^+ channels in ABA [4, 5, 8]; instead, they suggest that SNARE-dependent interactions and anchoring may be important to associate the K^+ channels with regulatory elements as part of a signaling protein scaffold. It will be of special interest now to identify the protein partners of these SNAREs and to explore the functional impact of channel clustering at the plant plasma membrane.

Experimental Procedures

Plant Growth, Protoplasts, and Transient Expression

Wild-type tobacco (*Nicotiana tabacum*) was grown and transfected either by infiltration with *Agrobacterium tumefaciens* or by biolistic delivery via 0.6 μm gold particles coated with the same expression plasmid DNA (5 μg DNA/60 mg gold) as described previously [7, 19]. Prior to cell fractionation and western blot analysis, hormone, inhibitor additions, and washout were by infiltration-mediated perfusion. Stock solutions of 20 mM ABA (Sigma, Poole UK) and 300 mM cycloheximide were prepared in ethanol and diluted 1000-fold for use in distilled water or in 5 mM Ca^{2+}-MES buffer (pH 6.1) with 0.1 mM KCl. 300 μM cycloheximide was found to suppress >90% of haKAT1-GFP expression, and ethanol diluted on its own to a final concentration of 0.1% (v/v) had no effect in control experiments (not shown).

Confocal Microscopy

Fluorescence was assessed 2 and 3 days after transfection after mounting leaf sections with Corning Medical Adhesive (Dow Corning, Midland MI) to a 1 ml custom-built chamber. Air-water boundaries that contribute to background fluorescence were eliminated by vacuum infiltration of the intercellular spaces. End-point experiments were carried out similarly by vacuum infiltration with ABA solutions. Otherwise, experiments were carried out under continuous superfusion after removing the upper epidermis and palisade cell layers. FM4-64 labeling was by superfusion with 5 μM dye solution for 5 min, and solution exchange times were determined by superfusion of leaf segments with propidium iodide. Confocal images were obtained as before [7] on a Zeiss LSM510-UV microscope (Zeiss, Jena, Germany) with 458 nm or 488 nm (GFP, FM4-64) and 514 nm (YFP) excitation and emitted light was collected through a NFT545 dichroic, 505–530 (GFP), 535–590 nm (YFP), and 560–615 nm (FM4-64) bandpass filters. Chloroplast fluorescence was detected with a 560 nm longpass filter and brightfield images were collected with a transmitted light detector. paGFP was photoactivated with 351 nm and 364 nm light from an 80 mW Enterprise II UV laser [7]. Stomatal apertures were determined from brightfield images after calibration. Numerical analysis was by nonlinear least-squares [38], and results are reported as means ± SE where appropriate.

Fractionation and Immunodetection

Total protein was extracted, and plasma membrane and internal membrane fractions were separated as described previously with leaves after transient transfection [7, 13]. Proteins were separated and western blots probed and analyzed as before [7] with radioactive [^{35}S, 0.5 μCi (18.5kBq)/ml] secondary antibody detected with a Fujifilm FLA5000 Phosphoimager (Raytek Scientific, Sheffield, UK).

Supplemental Data

Four figures and 11 movies are available at http://www.current-biology.com/cgi/content/full/17/16/1396/DC1/.

Acknowledgments

We are grateful to A. Honsbein, M. Boutry, and B. Lefebvre (Louvain, Belgium) for the H^+-ATPase PMA2:GFP construct, to I. Moore (Oxford, UK) for ST-YFP, to J. Vermeer and T. Munnik (Amsterdam, Netherlands) for YFP-FYVE, and to J. Denecke for BP80-YFP. This work was supported by BBSRC grants P13610, P12750, BB/D500595/1, a Wellcome VIP award, and John Simon Guggenheim Memorial Fellowship to M.R.B.

Received: March 13, 2007
Revised: July 11, 2007
Accepted: July 12, 2007
Published online: August 2, 2007

References

1. Jahn, R., Lang, T., and Sudhof, T.C. (2003). Membrane fusion. Cell *112*, 519–533.
2. Surpin, M., and Raikhel, N. (2004). Traffic jams affect plant development and signal transduction. Nat. Rev. Mol. Cell Biol. *5*, 100–109.
3. Sutter, J.U., Campanoni, P., Blatt, M.R., and Paneque, M. (2006). Setting SNAREs in a different wood. Traffic *7*, 627–638.
4. Blatt, M.R. (2000). Cellular signaling and volume control in stomatal movements in plants. Annu. Rev. Cell Dev. Biol. *16*, 221–241.
5. Hetherington, A.M., and Brownlee, C. (2004). The generation of Ca^{2+} signals in plants. Annu. Rev. Plant Biol. *55*, 401–427.
6. Peng, Z.Y., and Weyers, J.D.B. (1994). Stomatal sensitivity to abscisic acid following water-deficit stress. J. Exp. Bot. *45*, 835–845.
7. Sutter, J.U., Campanoni, P., Tyrrell, M., and Blatt, M.R. (2006). Selective mobility and sensitivity to SNAREs is exhibited by the *Arabidopsis* KAT1 K^+ channel at the plasma membrane. Plant Cell *18*, 935–954.
8. Schroeder, J.I., Allen, G.J., Hugouvieux, V., Kwak, J.M., and Waner, D. (2001). Guard cell signal transduction. Annu. Rev. Plant Physiol. Mol. Biol. *52*, 627–658.
9. Allen, G.J., Chu, S.P., Harrington, C.L., Schumacher, K., Hoffman, T., Tang, Y.Y., Grill, E., and Schroeder, J.I. (2001). A defined range of guard cell calcium oscillation parameters encodes stomatal movements. Nature *411*, 1053–1057.
10. van den Wijngaard, P.W.J., Sinnige, M.P., Roobeek, I., Reumer, A., Schoonheim, P.J., Mol, J.N.M., Wang, M., and de Boer, A.H. (2005). Abscisic acid and 14-3-3 proteins control K^+ channel activity in barley embryonic root. Plant J. *41*, 43–55.
11. Sutton, F., Paul, S.S., Wang, X.Q., and Assmann, S.M. (2000). Distinct abscisic acid signaling pathways for modulation of guard cell versus mesophyll cell potassium channels revealed by expression studies in *Xenopus laevis* oocytes. Plant Physiol. *124*, 223–230.
12. Roberts, S.K. (1998). Regulation of K^+ channels in maize roots by water stress and abscisic acid. Plant Physiol. *116*, 145–153.
13. Geelen, D., Leyman, B., Batoko, H., Di Sansabastiano, G.P., Moore, I., and Blatt, M.R. (2002). The abscisic acid-related SNARE homolog NtSyr1 contributes to secretion and growth: Evidence from competition with its cytosolic domain. Plant Cell *14*, 387–406.
14. Leyman, B., Geelen, D., Quintero, F.J., and Blatt, M.R. (1999). A tobacco syntaxin with a role in hormonal control of guard cell ion channels. Science *283*, 537–540.
15. Lefebvre, B., Batoko, H., Duby, G., and Boutry, M. (2004). Targeting of a *Nicotiana plumbaginifolia* H^+-ATPase to the plasma membrane is not by default and requires cytosolic structural determinants. Plant Cell *16*, 1772–1789.
16. Malinska, K., Malinsky, J., Opekarova, M., and Tanner, W. (2004). Distribution of Can1p into stable domains reflects lateral protein segregation within the plasma membrane of living *S. cerevisiae* cells. J. Cell Sci. *117*, 6031–6041.
17. Borner, G.H.H., Sherrier, D.J., Weimar, T., Michaelson, L.V., Hawkins, N.D., MacAskill, A., Napier, J.A., Beale, M.H., Lilley, K.S., and Dupree, P. (2005). Analysis of detergent-resistant membranes in *Arabidopsis*. Evidence for plasma membrane lipid rafts. Plant Physiol. *137*, 104–116.
18. Mongrand, S., Morel, J., Laroche, J., Claverol, S., Carde, J.P., Hartmann, M.A., Bonneu, M., Simon-Plas, F., Lessire, R., and Bessoule, J.J. (2004). Lipid rafts in higher plant cells—purification and characterization of triton X-100-insoluble microdomains from tobacco plasma membrane. J. Biol. Chem. *279*, 36277–36286.

19. Hurst, A.C., Meckel, T., Tayefeh, S., Thiel, G., and Homann, U. (2004). Trafficking of the plant potassium inward rectifier KAT1 in guard cell protoplasts of *Vicia faba*. Plant J. *37*, 391–397.
20. Vermeer, J.E.M., van Leeuwen, W., Tobena-Santamaria, R., Laxalt, A.M., Jones, D.R., Divecha, N., Gadella, T.W.J., and Munnik, T. (2006). Visualization of PtdIns3P dynamics in living plant cells. Plant J. *47*, 687–700.
21. Takano, J., Miwa, K., Yuan, L.X., von Wiren, N., and Fujiwara, T. (2005). Endocytosis and degradation of BOR1, a boron transporter of *Arabidopsis thaliana*, regulated by boron availability. Proc. Natl. Acad. Sci. USA *102*, 12276–12281.
22. daSilva, L.L.P., Taylor, J.P., Hadlington, J.L., Hanton, S.L., Snowden, C.J., Fox, S.J., Foresti, O., Brandizzi, F., and Denecke, J. (2005). Receptor salvage from the prevacuolar compartment is essential for efficient vacuolar protein targeting. Plant Cell *17*, 132–148.
23. Kotzer, A.M., Brandizzi, F., Neumann, U., Paris, N., Moore, I., and Hawes, C. (2004). AtRabF2b (Ara7) acts on the vacuolar trafficking pathway in tobacco leaf epidermal cells. J. Cell Sci. *117*, 6377–6389.
24. Ueda, T., Uemura, T., Sato, M.H., and Nakano, A. (2004). Functional differentiation of endosomes in *Arabidopsis* cells. Plant J. *40*, 783–789.
25. Very, A.A., and Sentenac, H. (2003). Molecular mechanisms and regulation of K^+ transport in higher plants. Annu. Rev. Plant Biol. *54*, 575–603.
26. Grabov, A., Leung, J., Giraudat, J., and Blatt, M.R. (1997). Alteration of anion channel kinetics in wild-type and *abi1-1* transgenic *Nicotiana benthamiana* guard cells by abscisic acid. Plant J. *12*, 203–213.
27. Simpson, F., Whitehead, J.P., and James, D.E. (2001). GLUT4—at the cross roads between membrane trafficking and signal transduction. Traffic *2*, 2–11.
28. Robert, S., Bichet, A., Grandjean, O., Kierzkowski, D., Satiat-Jeunemaitre, B., Pelletier, S., Hauser, M.T., Hofte, H., and Vernhettes, S. (2005). An *Arabidopsis* endo-1,4-beta-D-glucanase involved in cellulose synthesis undergoes regulated intracellular cycling. Plant Cell *17*, 3378–3389.
29. Russinovaa, E., Borst, J.W., Kwaaitaal, M., Cano-Delgado, A., Yin, Y.H., Chory, J., and de Vries, S.C. (2004). Heterodimerization and endocytosis of *Arabidopsis* brassinosteroid receptors BRI1 and AtSERK3 (BAK1). Plant Cell *16*, 3216–3229.
30. Robatzek, S., Chinchilla, D., and Boller, T. (2006). Ligand-induced endocytosis of the pattern recognition receptor FLS2 in *Arabidopsis*. Genes Dev. *20*, 537–542.
31. Paciorek, T., Zazimalova, E., Ruthardt, N., Petrasek, J., Stierhof, Y.D., Kleine-Vehn, J., Morris, D.A., Emans, N., Jurgens, G., Geldner, N., et al. (2005). Auxin inhibits endocytosis and promotes its own efflux from cells. Nature *435*, 1251–1256.
32. Penny, M.G., and Bowling, D.J.F. (1975). Direct determination of pH in the stomatal complex of *Commelina*. Planta *122*, 209–212.
33. Bowling, D.J.F. (1987). Measurement of the apoplastic activity of K^+ and Cl^- in the leaf epidermis of *Commelina communis* in relation to stomatal activity. J. Exp. Bot. *38*, 1351–1355.
34. Hille, B. (2001). Ionic Channels of Excitable Membranes, 3 edn. (Sunderland, MA: Sinauer Press).
35. Leonoudakis, D., Conti, L.R., Anderson, S., Radeke, C.M., McGuire, L.M.M., Adams, M.E., Froehner, S.C., Yates, J.R., and Vandenberg, C.A. (2004). Protein trafficking and anchoring complexes revealed by proteomic analysis of inward rectifier potassium channel (Kir2.x)-associated proteins. J. Biol. Chem. *279*, 22331–22346.
36. Leung, Y.M., Kang, Y.H., Gao, X.D., Xia, F.Z., Xie, H.L., Sheu, L., Tsuk, S., Lotan, I., Tsushima, R.G., and Gaisano, H.Y. (2003). Syntaxin 1A binds to the cytoplasmic C terminus of Kv2.1 to regulate channel gating and trafficking. J. Biol. Chem. *278*, 17532–17538.
37. Tian, G.W., Mohanty, A., Chary, S.N., Li, S.J., Paap, B., Drakakaki, G., Kopec, C.D., Li, J.X., Ehrhardt, D., Jackson, D., et al. (2004). High-throughput fluorescent tagging of full-length *Arabidopsis* gene products in planta. Plant Physiol. *135*, 25–38.
38. Marquardt, D. (1963). An algorithm for least-squares estimation of nonlinear parameters. J. Soc. Ind. Appl. Math. *11*, 431–441.
39. Meckel, T., Gall, L., Semrau, S., Homann, U., and Thiel, G. (2007). Guard cells elongate: relationship of volume and surface area during stomatal movement. Biophys. J. *92*, 1072–1080.
40. Shope, J.C., DeWald, D.B., and Mott, K.A. (2003). Changes in surface area of intact guard cells are correlated with membrane internalization. Plant Physiol. *133*, 1314–1321.
41. Ueda, T., Yamaguchi, M., Uchimiya, H., and Nakano, A. (2001). Ara6, a plant-unique novel type Rab GTPase, functions in the endocytic pathway of *Arabidopsis thaliana.* EMBO J. *20*, 4730–4741.